

## Article

# Evaluation of Rotational Stability and Stress Shielding of a Stem Optimized for Hip Replacements—A Finite Element Study

Mario Ceddia \* and Bartolomeo Trentadue 

Department of Mechanics, Mathematics and Management, Politecnico di Bari University, 70125 Bari, Italy; bartolomeo.trentadue@poliba.it

\* Correspondence: marioceddia1998@gmail.com

**Abstract:** The natural distribution of stress in the femur is altered when total hip arthroplasty (THA) is performed. In fact, when a stem is inserted inside the femur, there is a variation in stress due to the difference in rigidity between the material with which the stem is made and the femur. This generates the phenomenon of stress shielding. The aim of this study is to design an optimized prosthesis that guarantees an excellent rotational stability and a reduced stress shielding. **Methods:** Through the finite element method (FEM), the mechanical behavior of the stem subjected to the loads described by ISO 7206-4:2010 is studied. **Results:** Through topological optimization, there is a reduction in stress shielding in the proximal zone of 31.46%. The addition of ridges on the dorsal side of the stem also improves rotational stability by 27.82%. **Conclusions:** The decrease in stiffness that is recorded with the optimized stem guarantees a greater distribution of stress on the bone. The presence of dorsal ridges also favors the corticalization of the bone as it loads the bone near the dorsal, ensuring further stability. The perforated prosthesis presented in this study shows an increase in primary stability and an improvement in rotational stability as there is also a bone regrowth inside the prosthesis.

**Keywords:** prosthesis; stress shielding; topological optimization; FEM analysis



**Citation:** Ceddia, M.; Trentadue, B. Evaluation of Rotational Stability and Stress Shielding of a Stem Optimized for Hip Replacements—A Finite Element Study. *Prosthesis* **2023**, *5*, 678–693. <https://doi.org/10.3390/prosthesis5030048>

Academic Editors: Giuseppe Solarino and Umberto Cottino

Received: 27 June 2023

Revised: 14 July 2023

Accepted: 18 July 2023

Published: 26 July 2023



**Copyright:** © 2023 by the authors. Licensee MDPI, Basel, Switzerland. This article is an open access article distributed under the terms and conditions of the Creative Commons Attribution (CC BY) license (<https://creativecommons.org/licenses/by/4.0/>).

## 1. Introduction

Total hip arthroplasty (THR) is the therapy to treat degenerative diseases, such as hip osteoarthritis or degenerative cartilage diseases and trauma. In the case of trauma, intracapsular fractures may be found at the level of the head, intratrochanteric, included in the area between the small and the great trochanter and subtrochanter, at the diaphyseal level [1]. The purpose of a hip replacement is to restore the motility and functionality of the joint without causing pain to the patient. Both the stem and the components that make up the joint must be designed to ensure long-term mechanical reliability and reliability at the implantation site [2]. The use of THR is increasing, particularly in young patients. This factor influences the number of revision surgeries, as the increased life expectancy of the younger population has led to an increase in revision surgeries. In revision surgery, numerous technical difficulties are encountered due to bone loss as a result of mobilization [3]. The search for prosthetic alternatives has led to the modification of the primary components, the introduction of improvements and the changes made to obtain a more proximal load transfer to the femur in order to reduce the phenomenon of stress shielding [4–7] and therefore preserve the bone for possible revision surgery. In the last two decades, several conservative femoral prostheses have been designed and some authors have supported their use [1,2]. Traditionally, tapered anatomical or cylindrical types are used. The classic tapered stem has a rectangular cross-section, four corners and four flat surfaces that are compressed in the proximal femur, whereas in the second type, the stem in the mid-distal view follows the curvature of the femoral canal [8–12]. The anatomy of the femur, in fact, has two kinds of curvatures called curved and procurvate (Figure 1).

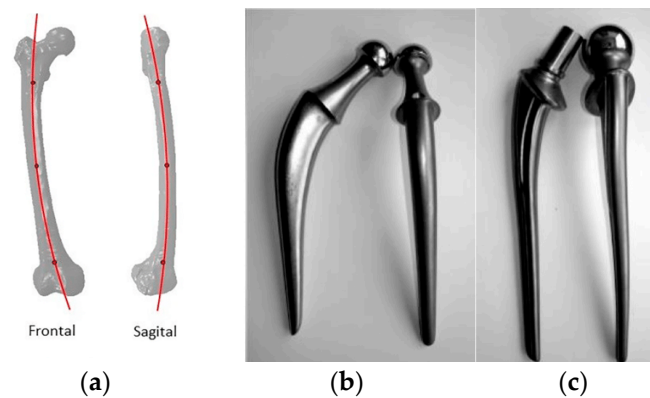


**Figure 1.** (a) Curvature of the femur in frontal and sagittal view; (b) right stem; (c) curved stem.

Studies comparing right and curved stems have shown that curved stems have a greater torsional stability, both proximal and distal [8]. The torsional stability of the anatomical stems has also been shown, and it is not proportional to the length of the stem itself. Despite the positive results of long-stem femoral prostheses, there are still concerns about the relatively high rate of early periprosthetic fractures, pain in the front of the thigh, bone loss and high skin stress [13–15], mainly due to stress shielding and rotational instability. The aim of this study is to simultaneously evaluate the effect of stiffness change on stress shielding and rotational stability.

### 1.1. Rotational Instability

Rotational instability is a problem that is noted in many revisions. The result of the forces acting on the femoral head is found to be eccentric with respect to the axis of the stem, thus exerting a high torsional moment to the prosthesis during walking, exposing it to rotational stresses as well as compression, flexion and traction stresses (Figure 2).

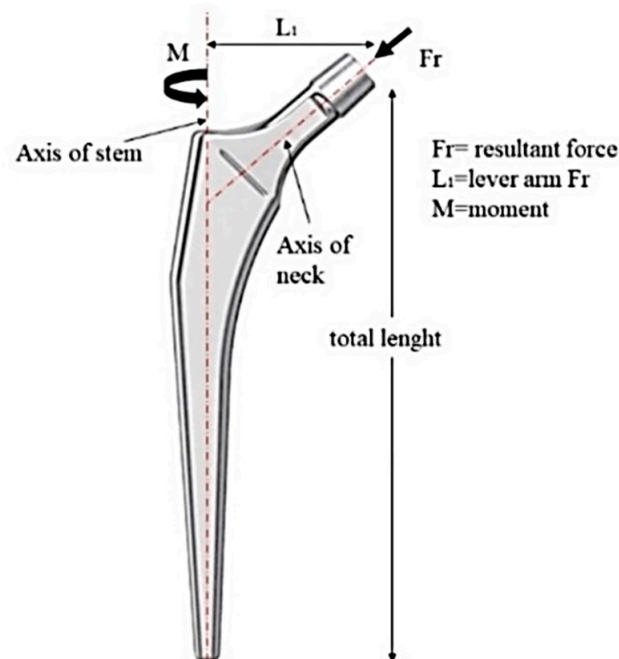


**Figure 2.** Direction of application loads and moments.

Sections of the stem with carvings or with edges improve the anchorage of the stem. For example, rectangular sections with horizontal grooves (Figure 3a) and vertical ones ensure the anchorage of the stem to several points of the proximal cortical.

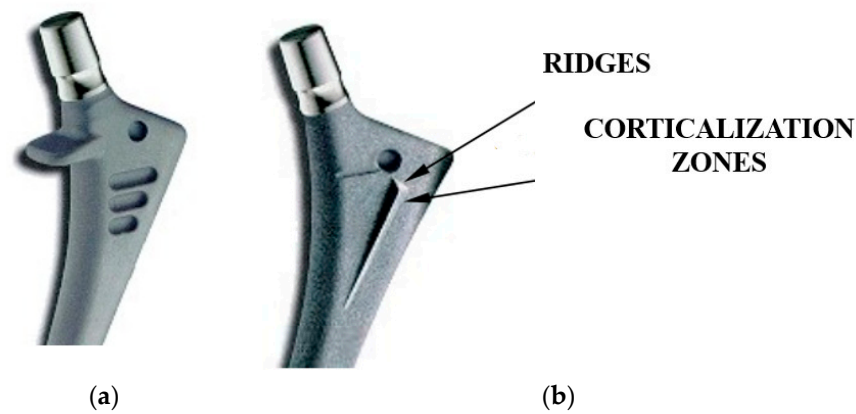


**Figure 3.** (a) Sheet with horizontal grooves, (b) stem with ridges.

Thanks to the overstresses induced by both the notch sections and grooves, bone regrowth is stimulated, which favors the anchoring of the stem. In the same way, the presence of ridges on the stem in Figure 3b increases the stresses on the surrounding spongy bone, whereby corticalization creates islands of cortical bone that stabilize the prosthesis.

$$F_2 = \frac{M}{L_2} \tag{1}$$

where:

$F_2$ = force transmitted to the bone;  
 $L_2$ =lever arm of  $F_2$ .

Rotational stability is defined as the resistance of the implant to the joint forces that induce rotation around the longitudinal axis of the implant. Walking, climbing stairs and rising from a sitting position cause moment  $M$  around the axis of the stem Figure 4. According to Equation (1), the lever arm  $L_2$  depends on various anatomical configurations used (Figure 5).

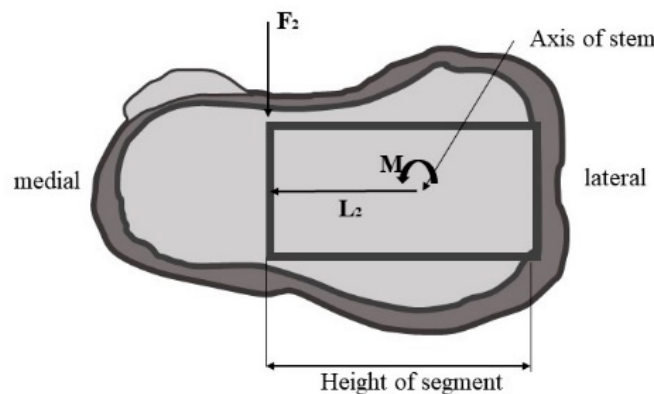


**Figure 4.** Torsional moment ( $M$ ) produced by the introduced force ( $F_2$ ) and the active lever arm ( $L_2$ ).

It can be seen that the greater the lever arm ( $L_2$ ) the lower the force ( $F$ ) transmitted to the bone; and contrariwise, the smaller the lever arm ( $L_2$ ), the greater the force ( $F$ ) transmitted to the bone. Prostheses with a reduced radius ( $L_2$ ) are not as strong because they produce a higher surface load, leading to early prosthetic failure caused by local overload per unit area ( $N/mm^2$ ). A large medial and/or lateral radius produces greater resistance to rotation. The cortical support of the prosthesis is indispensable for the stability and transmission of force, since the larger the area, the lower the specific surface load. The spongy bone is a dynamic element of minor importance in this sense since it yields when subjected to a specific axial load. Studies carried out [16] have shown that the design of

the stem in the proximal zone plays a fundamental role in ensuring rotational stability. Stems with rectangular or trapezoidal sections have better behaviors in terms of stability to rotation because they provide greater anchoring surfaces than oval or elliptical shapes.

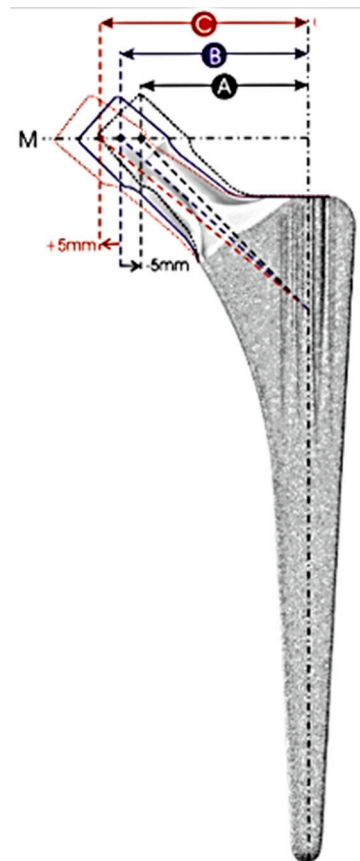


**Figure 5.** Lever arm configuration.

### 1.2. Stress Shielding

According to Wolff's law, [16–32] bone remodeling occurs to adapt bone structure and geometry to loads acting from the outside. Before the implant is inserted into the femur, all the load is discharged along the bone surfaces, and after the insertion of the prosthesis, the bone is found to be subjected to lower stresses. What occurs is an uneven distribution of stresses since we have the upper part of the femur, which undergoes less loads, while the distal part is overstressed through compression by the presence of the stem. Figure 6 shows that bone density decreases when the stress acting on the bone is lower than the physiological stress [33]. While it increases, the acting loads are found to be higher. This phenomenon is mainly due to the difference between the stiffness of the implant and that of the femur. The implants are made of metal alloys (steel, cobalt–chrome, titanium), which are more stiff (100–200 Gpa) compared to that of the human femur (1–30 GPa) [34,35].

Therefore, in order to resolve the problem of stress shielding, it is necessary to ensure that there is a decrease in the stiffness of the stem so as to have an increase in the transfer of the load to the bone, as also observed by Diegel et al. [35]. The stiffness is found to be dependent on the section and the material. In this study, we will vary the stiffness by acting on the section, and through the finite element method, we will compare the stiffness expressed by Equation (2) of a modified stem, with the stiffness of a traditional solid stem:

$$\text{Rigidness} = \frac{\text{Applied load}}{\text{Displacement}} \quad (2)$$

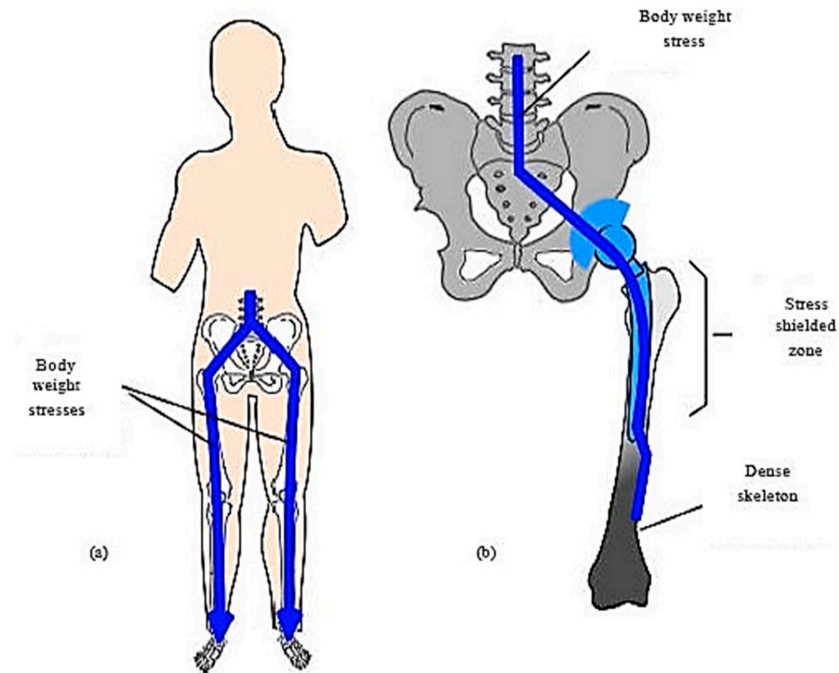


**Figure 6.** Simple scheme of stress shielding [35]. (a) force transfer along the femur, (b) force transfer along the stem.

In addition, stress shielding will be evaluated by comparing the von Mises stress of the intact cortical bone with the von Mises stress of the cortical bone with the implant ( $\sigma^{intact\ bone}$  and  $\sigma^{bone\ with\ implant}$ , respectively). Fraldi and Esposito [36] defined stress shielding (SS) according to Equation (3):

$$SS = \frac{\sigma^{intact\ bone} - \sigma^{bone\ with\ implant}}{\sigma^{intact\ bone}} \quad (3)$$

A low SS reflects the changes in local stress in a region after implantation. A positive SS implies that the local region undergoes less stress than pre-surgical conditions, which induces stress shielding. A negative SS suggests instead an increase in local stress or a potential concentration of stress. Rotational stability will be studied through the evaluation of stem rotations within the femur and comparing these results with those reported in the literature [37]. This study hypothesizes that comparing a traditional solid stem to an optimized Figure 7 stem will effectively reduce the effect of stress shielding and improve rotational stability. Moreover, thanks to the finite elements, important results can be obtained that provide the designer with the recommendations to be adopted to ensure implant stability.

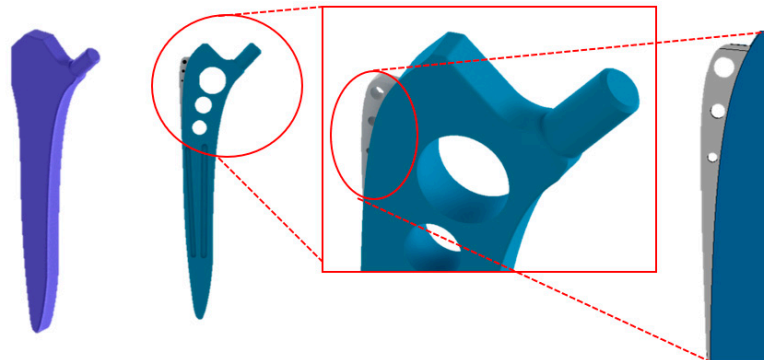


**Figure 7.** On the left, a traditional full-stem prosthesis with rectangular section; on the right, prosthesis with minimization in the proximal area having holes, ridges and slots to improve rotation stability.

## 2. Materials and Methods

### 2.1. Evaluation of Stem Stiffness

The finite element models were created in accordance with the load and constraint requirements of ISO 7206-4:2010. This standard provides a good indication of the ability that the femoral prosthesis possesses to withstand load conditions. ANSYS® Workbench software was used for finite element simulation (Figure 8). The finite element analysis (FEA) model includes a suppression block (transmits 2300N compression to the stem), a femur head and the implant embedded in the cement 80 mm away from the center of the femoral head with an adduction angle of 10° and a flexion of 9°. Both were made and assembled with 3D Inventor software. For the above parts, the material properties used in FEA are given in Table 1. The type of delimited contact was defined for bone cement—implant and conical head of the implant—the inner surface of the femoral head, and the outer surface of the head. The concrete block was constrained in all directions. For all parts of the FEA model, tetrahedral elements with an average element size of 2 mm were used.

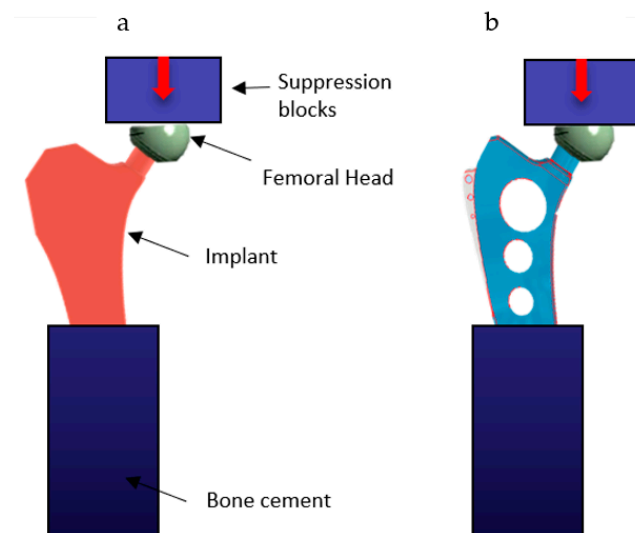


Figure 8. FEM model of ISO 7206-4 test: (a) standard stem, (b) optimized stem.

Table 1. Mechanical properties of various materials.

Material	Modulus of Elasticity	Shear Modulus (Gpa)	Poisson's Ratio	Compressive Strength (Mpa)	Yield Strength (Mpa)	Density g/cm <sup>3</sup>
Cortical bone	Ex = 6979 (Mpa) Ey = 18,132 (Mpa) Ez = 6979 (Mpa)	Gyz = 5.6 Gzx = 4.5 Gxy = 6.2	$\nu_{yz} = 0.25$ $\nu_{zx} = 0.4$ $\nu_{xy} = 0.25$	195		2.02
Cancellous bone	Ex = 660 (Mpa) Ey = 1740 (Mpa) Ez = 660 (Mpa)	Gyz = 0.211 Gzx = 0.165 Gxy = 0.260	$\nu_{yz} = 0.25$ $\nu_{zx} = 0.4$ $\nu_{xy} = 0.25$	16		1.37
Ti6Al4V	110 (GPa)		0.3	970	930	4.42
Steel (suppression blocks)	210 (Gpa)		0.3			
Bone cement	3.8 (Gpa)		0.3			
Cr-Co (femoral head)	200 (Gpa)		0.33			

### 2.2. Bone Implant Stress Assessment

To model the stem inserted inside the femur, a cylindrical 3D model (Figure 9) was prepared, dividing it into the cortical and spongy part [32]. Once assembled, the model was converted into an .stp file and exported to Ansys Workbench to prepare the mesh, define the contact and set boundary conditions. The assembled model consists of 3 parts (cortical bone, spongy bone, femoral stem); this classification of the CAD model served to assign the properties of the material independently. It was assumed that both cortical

and spongy bones had linear, orthotropic and homogeneous mechanical properties. The bone properties listed in Table 1 were taken from [33–35]. As for the stem, it was made of Ti6Al4V titanium alloy. The properties of titanium alloy are shown in Table 1. The base of the bone model was constrained in all directions. The contacts between prostheses and bones were set as: bonded and no separation. The loads were taken from the work of Chen et al., 2014 [38], and Bergmann et al., respectively [39] (Figure 10).

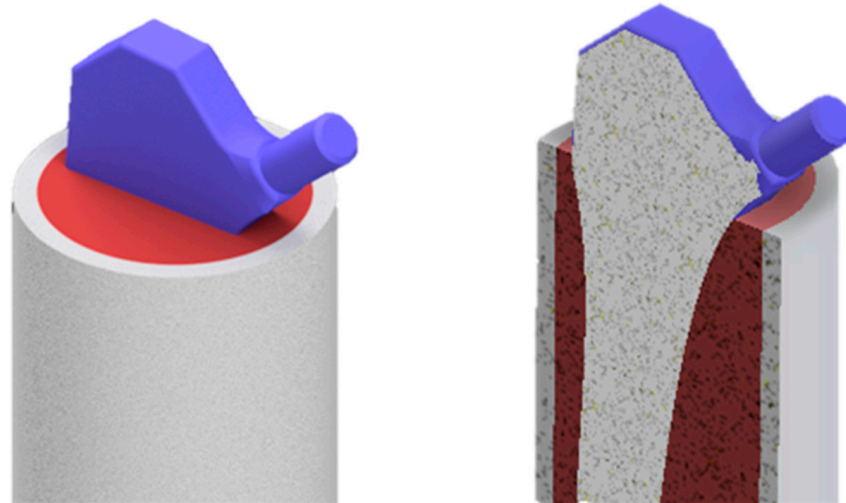


**Figure 9.** Representative model of the stem inserted into the femur; cortical thickness considered 3 mm.

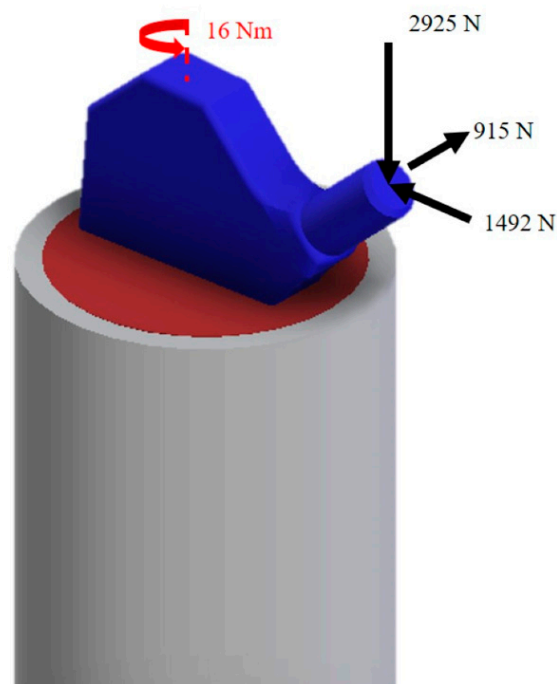


**Figure 10.** The direction and application of loads and time for the numerical model studied [38].

### 2.3. Meshing

The stem-bone model was assembled with approximately 614,904 tetrahedral elements (Figure 11), adopting an average element size of 2.4 mm, as also reported in [38], for the stem. Instead, with regard to the bone (since it is the main object of the study), within which we aimed to investigate the distribution of tensions, a mesh size of 2 mm was adopted to produce a greater accuracy in the results.

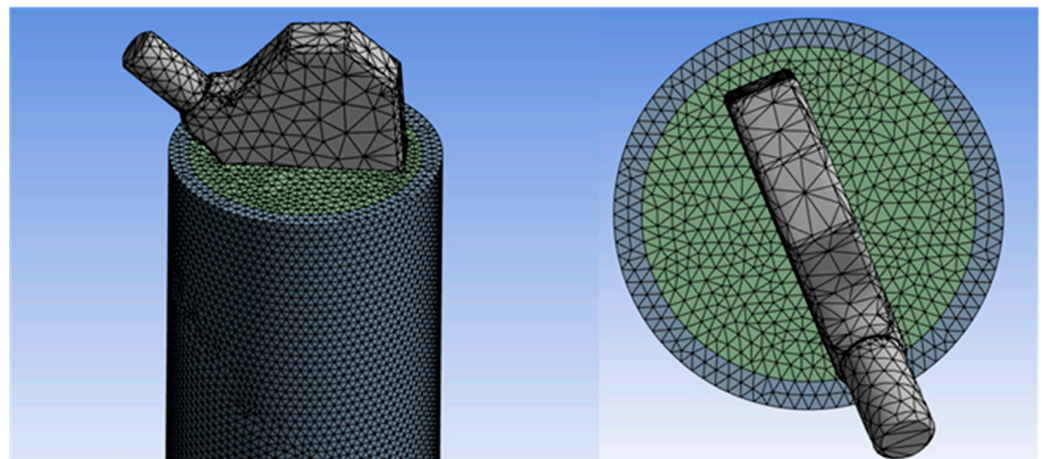


**Figure 11.** Mesh characteristics used: for the stem size = 2.4 mm; for the bone size = 2 mm.

Figure 12 shows the mesh convergence verification that displays how adopting an element size of 2 mm resulted in a committed error of 0.20% [38,39]. Mesh convergence analysis is an important process in finite element analysis (FEA) to ensure the accuracy and reliability of results. Mesh convergence refers to achieving stable and consistent results as the mesh size and density are refined. If the results do not converge as expected, a repetition of the meshing process and an analysis with a different strategy may be needed to achieve adequate convergence. This could include the use of localized mesh refinement techniques or an optimization of analysis parameters.

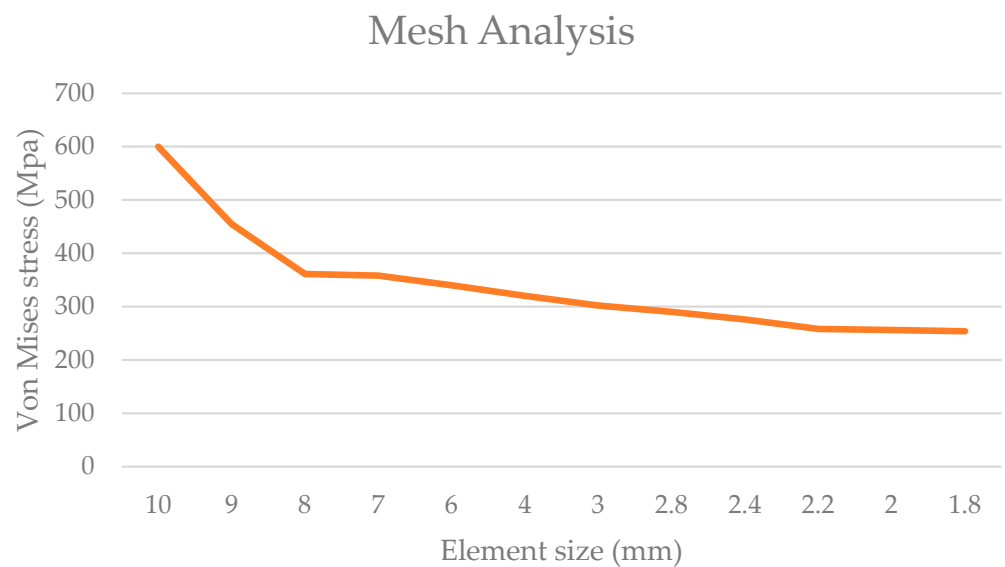


**Figure 12.** Mesh convergence analysis between element dimension and von Mises stress.

### 3. Results

Figure 13 shows the displacement load graph and the stiffness obtained with the first FEM model (ISO 7206-4:2010) according to Equation (4) for the standard stem and for the optimized one, comparing them with that of the human femur [40].

Based on these early stiffness results, we can expect the stem femur in Ti6Al4V to have a lower stress after THA, as the Ti6Al4V stem is stiffer than the femur, whereas the femur with the optimized stem can instead present opposing results, in which a greater stress is expected after THA. Through the second FEA study, in Figure 14, the results of the von Mises stress for the traditional and optimized stems are reported.

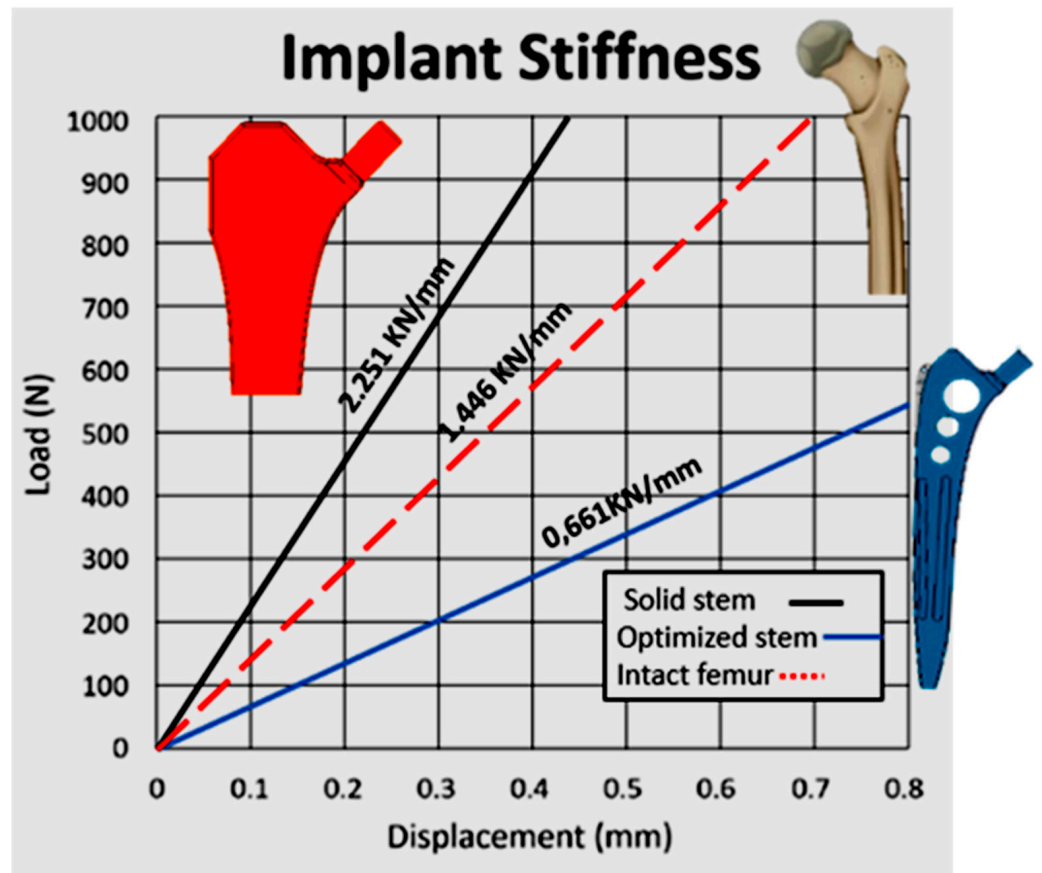


Figure 13. Load–displacement graph for Ti6Al4V stem, optimized stem and intact femur. The stiffness value of each configuration is presented above the respective slopes on the diagram.

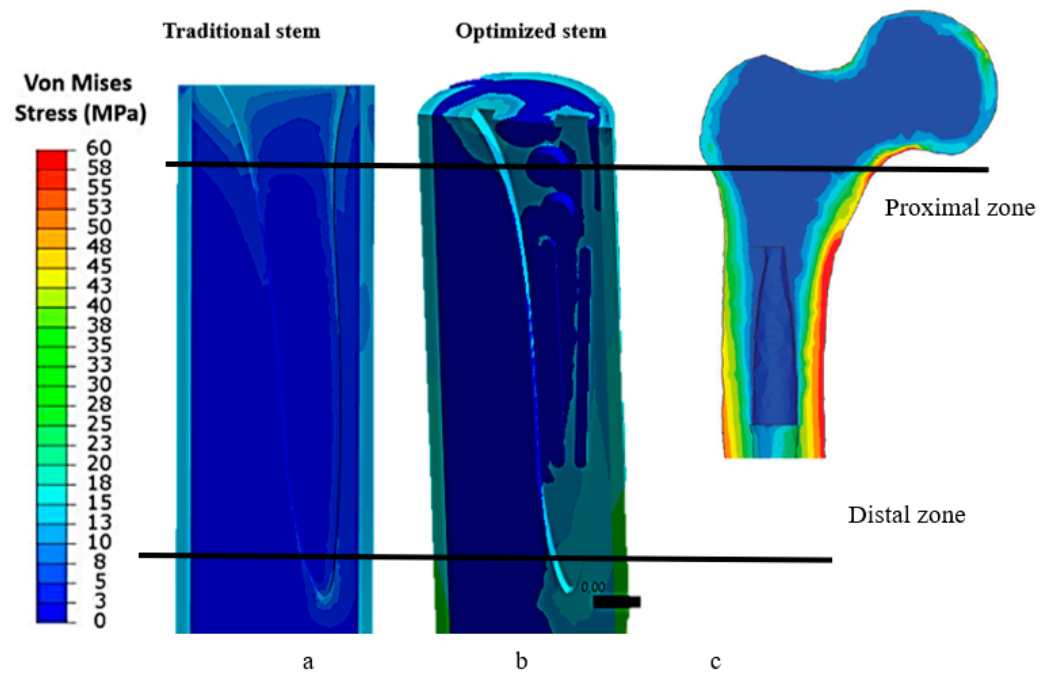


Figure 14. Von Mises stress distribution on bone: (a) traditional stem; (b) optimized stem; (c) intact bone [34].

Regarding the stems, in Figure 15, the results of the von Mises stress are reported.

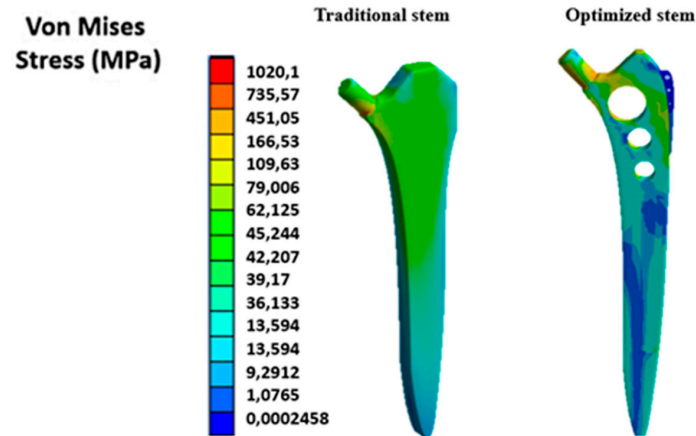


Figure 15. Von Mises stress for stems.

As shown in Figure 14, stress is mainly concentrated in the proximal zone, as is also shown by Swanson et al. [41]. Observing the distribution of stress for the full stem and the optimized stem, it is clear that there is a global increase in stress from the proximal to the distal zone. This phenomenon can also be explained by observing Figure 15, in which we see how the optimized stem has a lower stress than the traditional solid stem; this phenomenon makes it clear how a part of the load is distributed more on the bone in contact, with a reduction in stress shielding. Moreover, by considering the yield stress (110 Mpa) of the cortical bone detected by a study on cadavers [42], we can affirm that the insertion of the prostheses does not involve the risks of fracture for the femur.

Through Equation (3), we can calculate the stress shielding for the two stems (Table 2), taking as reference the von Mises stress of the stemless bone (Figure 14) and the results of the von Mises stress for the bone in the two cases, as summarized in Figure 16.

Table 2. Reduction in stress shielding for the three zones: proximal, central, distal.

von Mises Bone Stress with Traditional Stem	von Mises Bone Stress with Optimized Stem	Stress Shielding Reduction %	
		Traditional Stem	Optimized Stem
Proximal 13 Mpa	Proximal 17 Mpa	24.08%	31.46%
Central 3.1 Mpa	Central 4.2 Mpa	5.54%	7.5%
Distal 4.6 Mpa	Distal 5 Mpa	9.59%	10.1%

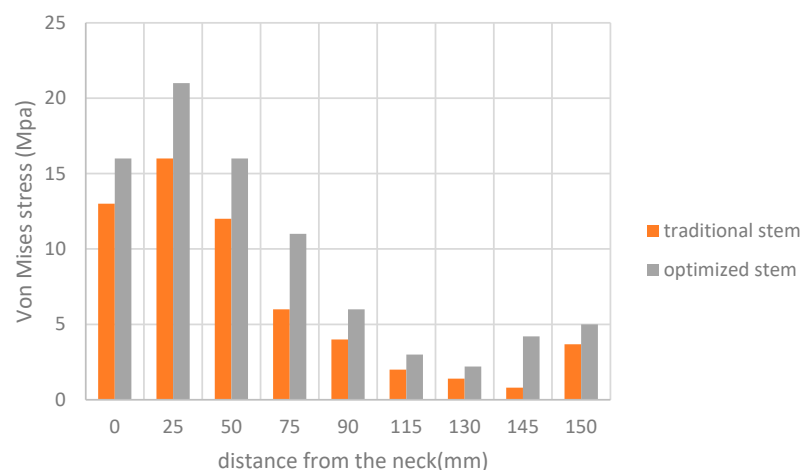
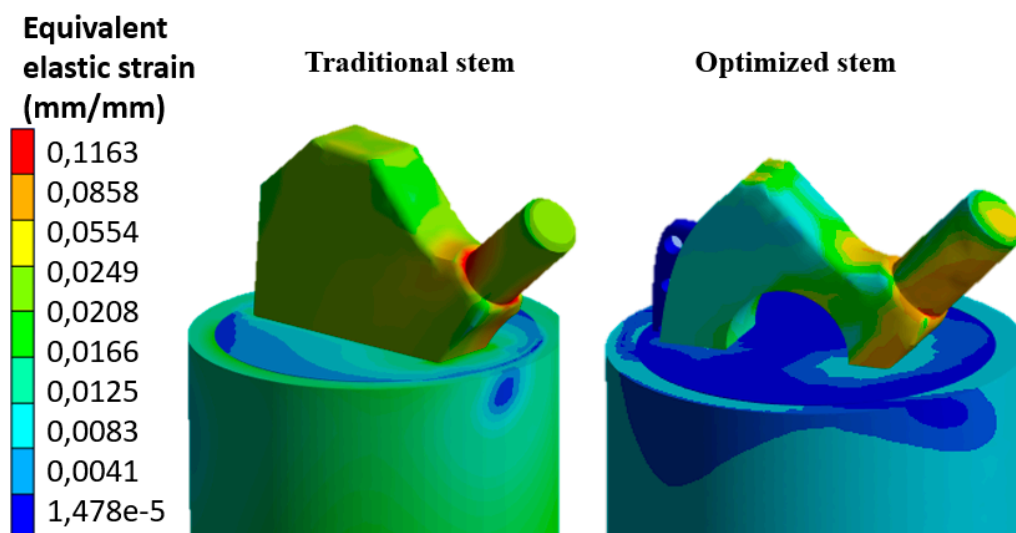


Figure 16. Trend of von Mises stresses in the bone.

From Table 2, it can be seen how, in the proximal area where there are higher loads, with the optimized stem, we obtained a reduction in stress shielding at 31.47% compared to the traditional stem at 24.08%. This result is also a part of the percentages obtained from other studies in the literature [43–46].

Figure 17 shows the deformation of the stem in the bone.



**Figure 17.** Equivalent deformation of the implant.

Micromovements of femoral prostheses refer to the small sliding or rotational movements that can occur between the femoral stem of the prosthesis and the surrounding bone after implantation. These movements can be influenced by various factors, including implant design, bone fixation, the characteristics of the patient's bone and physical activity. The goal of implanting a femoral prosthesis is to achieve adequate stability and integration with the surrounding bone. However, it is not always possible to completely avoid micromovements. Some micromovements can be considered normal and can help in the stimulation of bone growth and osseointegration of the implant. However, excessive or uncontrolled movements can lead to problems such as the premature wear of the implant, the detachment of the coating or the overall instability of the implant. Therefore, it is important to try to minimize unwanted micromovements during the design and implantation of femoral prostheses. The maximum displacement values of the center of the head are 0.023 mm for the standard stem and 0.0166 mm for the optimized stem, thus reducing torsional deformation by 27.82%. It is therefore clear that the optimized prosthesis has a greater rotational stability than the standard prosthesis. This can be explained by considering that during the insertion of the standard stem, the greater trochanter was found to be weakened more due to the design of the proximal zone of the stem. Therefore, the optimized stem has a less invasive design, which preserves the trochanter, which, in contact with the stem, provides greater stability.

## 4. Discussion

### 4.1. Effect of Stem Stiffness

The stiffness of the femoral stem of a prosthesis is an important factor to consider in the design and choice of the implant: it can influence the load transferred to the surrounding bone and the overall mechanical behavior of the implant. The stiffness of the femoral stem depends on several factors. (1) Materials: Different metallic materials, such as titanium alloys or stainless steel, present different stiffness characteristics. For example, titanium has a greater ductility than stainless steel, which can affect the overall stiffness of the stem. (2) Geometry: A stem with a larger diameter or a larger cross-section will have greater stiffness than one with a smaller diameter. In addition, the stem can be designed with

a cylindrical, conical or modular geometry, which will affect its overall stiffness. Bone fixation, for example, is a kind of cemented stem which has a greater rigidity than a stem with press-fit fixation, since acrylic cement contributes to the overall rigidity of the stem. The choice of fixation method depends on the characteristics of the patient's bone and the preferences of the surgeon. (3) Stem–bone interface: The interaction between the femoral stem and the surrounding bone can affect the overall stiffness of the implant. For example, if the stem is designed with a porous surface or hydroxyapatite coating, this can promote osseointegration and increase the stability of stem–bone contact, thus affecting overall stiffness. It is important to carefully consider the stiffness of the femoral stem according to the specific needs of the patient [47]. Excessive stiffness of the stem could cause excessive stress on the surrounding bone, while insufficient stiffness could compromise the stability of the implant.

#### 4.2. Optimization of Stem–Femur Contact

There are several factors to consider when optimizing the contact between the femoral stem and the bone [31,48,49]. (1) Stem profile design: The geometry of the stem profile can affect contact with the surrounding bone. Several designs of femoral stems are currently available, including cylindrical, conical or anatomical stems. The choice of stem profile depends on the anatomical features of the patient and the condition of the femur bone. (2) Surface coatings: Some femoral dentures may have special surface coatings to improve contact with the bone. For example, the coating of hydroxyapatite or other porous coatings can promote bone growth and promote a better integration of the implant with the bone. (3) Bone fixation: Implant stability can be improved through bone fixation techniques, such as the use of acrylic cement or press-fit fixation. The method of fixation depends on the characteristics of the patient's bone and the design of the prosthesis. (4) Dimensional adaptation: It is important that the size of the femoral stem is appropriate for the medullary canal of the bone [50]. Proper adaptation avoids excessive stress on the walls of the surrounding bone and promotes the stability of the implant. (5) Load and activity: Optimizing contact between the femoral shaft and bone also requires a consideration of the patient's load and activities. The stem design and material must be able to withstand the mechanical stresses associated with everyday activities, such as walking, climbing stairs and other movements. It is important that the contact between the femoral shaft and the bone is stable and long-lasting to ensure the good functionality of the prosthesis and reduce the risk of complications, such as implant failure or a detachment of the coating. If sufficient adaptation is not achieved, the phenomenon of stress shielding is generated [47]. Therefore, the distal part must be flexible to transfer loads to the bone. Solid sections have the disadvantage of stiffening the stem and presenting maximum torsional instability, while grooved or windowed sections increase the flexibility of the stem and guarantee torsional stability. The stiffness of the stem, which is determined by the geometry of its cross-section and elastic modulus, affects the stresses in the entire system. Studies show that it is possible to achieve a reduction in stress shielding with hollow section stems compared to solid stems, as some hollow forms work better than others [36]. The advantage of the hollow stem lies in the greater rigidity control while maintaining acceptable anatomical adaptation. This is possible thanks to the wide range of rigidities offered by hollow sections. The external shape of the stem can be chosen according to anatomical criteria and the internal dimensions can be adjusted to optimize bone stresses. In any case, it is necessary to find a compromise to optimize both the stability and flexibility of the prosthesis. In fact, as reported in [48], a reduction in stem stiffness certainly leads to a reduction in stress shielding, but also to an increase in stress in the proximal area of the femur, inducing the risk of fractures. Figure 18.

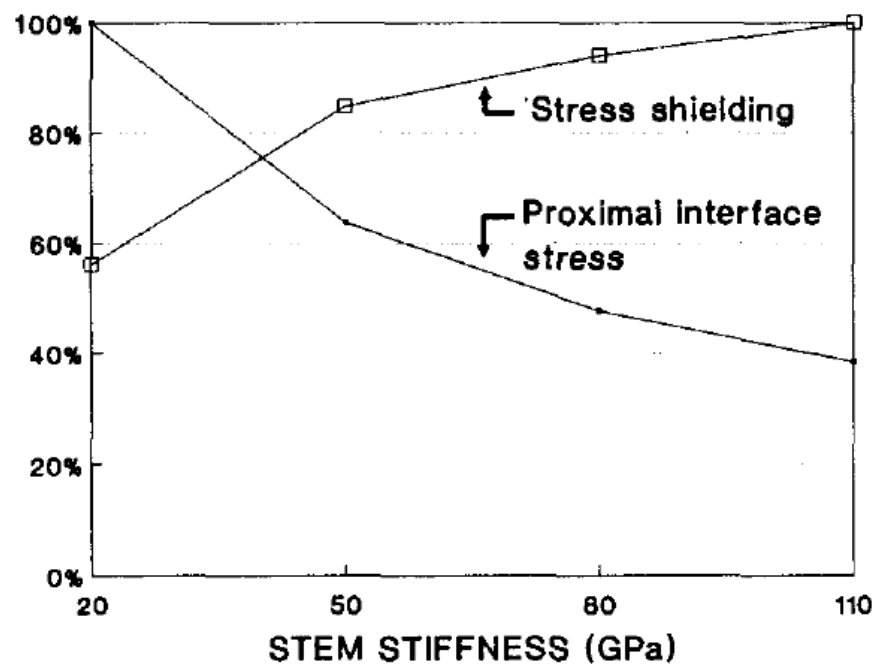


**Figure 18.** Relative relationships between stress shielding and stress of the proximal interface with stem stiffness. This chart clearly illustrates the main design conflict.

Proximally wide prostheses have a greater prosthetic support and therefore a greater rotational stability. In fact, as explained in [31], the proximal segment height exerts a greater load on the bone surface; when the resistance to rotation is exceeded, the torque can no longer be transmitted completely to the bone, and the stem begins to rotate. Consequently, a low-transmitted moment is indicative of a lower rotational stability. Torsional resistance can be increased in relation to femoral neck geometry [49] and by adding ridges on the lateral surfaces of the stem. The addition of ridges anteriorly, posteriorly and laterally increases rotational stability by 50% [50]. When porously coated implants are used, rotational stability is guaranteed only if the diaphysis is under boring and very narrow diaphyseal fixation is achieved [51]. The current study, conducted with the finite element method (FEA), is limited by the use of mechanical properties of materials found in the literature. But upon comparing the results obtained with those performed by other scholars [44,45,52,53], we note a certain numerical correspondence; in fact, in this study, a reduction of about 32% was achieved with regard to stress shielding, compared to 15–40% obtained by other studies.

## 5. Conclusions

This study outlined a new single-stem design for the (THR) through finite element modeling to reduce the phenomenon of stress shielding leading to aseptic loosening and improve rotational stability. It has been shown that by using a prosthesis with holes and windows, stiffness can be greatly reduced and stress shielding can suffer a decrease of 31.46% compared to 24.08% of the complete stem. This study also showed that drilling transverse holes in the prosthesis improves rotational stability by 27.82% compared to the full stem, as bone regrowth both on the surface and inside the prosthesis would improve stability. The current study conducted with the finite element method (FEA) is limited by the use of mechanical properties of materials found in the literature. But comparing the results obtained with those performed by other scholars [44,45,52,53], we note a certain numerical correspondence; in fact, in this study, a reduction of about 32% was achieved with regard to stress shielding, compared to 15–40% obtained by other studies. The strength of this study is that, thanks to the FEM method, it is possible to quickly carry out evaluations that can improve the behavior of the stem. Future studies should consider the effect of bone growth on the stem and physiological loads.

**Author Contributions:** Conceptualization, M.C. and B.T.; methodology, M.C.; software, M.C.; validation, B.T.; formal analysis, M.C. and B.T.; investigation, M.C.; resources, M.C. and B.T.; data curation, M.C.; writing—original draft preparation, M.C. and B.T.; writing—review and editing, M.C., B.T.; visualization, B.T.; supervision, B.T.; project administration, B.T. All authors have read and agreed to the published version of the manuscript.

**Funding:** This research received no external funding.

**Institutional Review Board Statement:** Not applicable.

**Informed Consent Statement:** Not applicable.

**Data Availability Statement:** All experimental data to support the findings of this study are available upon request to the corresponding author.

**Conflicts of Interest:** The authors declare no conflict of interest.

## References

1. Yang, S.; Liu, Y.; Ma, S.; Ding, C.; Kong, Z.; Li, H.; Huang, F.; Chen, H.; Zhong, H. Stress and strain changes of the anterior cruciate ligament at different knee flexion angles: A three-dimensional finite element study. *J. Orthop. Sci.* **2023**, *in press*. [[CrossRef](#)]
2. Rani, S.; Jain, N.; Barua, S.L.; Idnani, S.; Kaushik, N. Stress analysis in implant, abutment, and peripheral bone with different restorative crown and abutment materials: A three-dimensional finite element analysis study. *Dent. Res. J.* **2023**, *20*, 62. [[CrossRef](#)]
3. Wei, W.; Wang, T.; Liu, J.; Mao, K.; Pan, C.; Li, H.; Zhao, Y. Biomechanical effect of proximal multifidus injury on adjacent segments during posterior lumbar interbody fusion: A finite element study. *BMC Musculoskelet Disord.* **2023**, *24*, 521. [[CrossRef](#)] [[PubMed](#)]
4. Kovuru, V.; Aileni, K.R.; Mallepally, J.P.; Kumar, K.S.; Sursala, S.; Pramod, V. Factorial analysis of variables affecting bone stress adjacent to mini-implants used for molar distalization by direct anchorage—A finite element study. *J. Orthod. Sci.* **2023**, *12*, 18.
5. Rometsch, E.; Bos, P.K.; Koes, B.W. Survival of short hip stems with a “modern”, trochanter-sparing design—A systematic literature review. *Hip Int.* **2012**, *22*, 344–354. [[CrossRef](#)]
6. Banerjee, S.; Pivec, R.; Issa, K.; Harwin, S.F.; Mont, M.A.; Khanuja, H.S. Outcomes of short stems in total hip arthroplasty. *Orthopedics* **2013**, *36*, 700–707. [[CrossRef](#)]
7. Moskal, J.T.; Capps, S.G. Is limited incision better than standard total hip arthroplasty? A meta-analysis. *Clin. Orthop. Relat. Res.* **2013**, *471*, 1283–1294. [[CrossRef](#)] [[PubMed](#)]
8. Berstock, J.R.; Blom, A.W.; Beswick, A.D. A systematic review and meta-analysis of the standard versus miniincision posterior approach to total hip arthroplasty. *J. Arthroplast.* **2014**, *29*, 1970–1982. [[CrossRef](#)] [[PubMed](#)]
9. Yue, C.; Kang, P.; Pei, F. Comparison of direct anterior and lateral approaches in total hip arthroplasty: A systematic review and meta-analysis (PRISMA). *Medicine* **2015**, *94*, e2126. [[CrossRef](#)]
10. Feyen, H.; Shimmin, A.J. Is the length of the femoral component important in primary total hip replacement? *Bone Jt. J.* **2014**, *96*, 442–448. [[CrossRef](#)]
11. Khanuja, H.S.; Banerjee, S.; Jain, D.; Pivec, R.; Mont, M.A. Short bone-conserving stems in cementless hip arthroplasty. *J. Bone Jt. Surg. Am.* **2014**, *96*, 1742–1752.
12. Courpied, J.P.; Caton, J.H. Total hip arthroplasty, state of the art for the 21st century. *Int. Orthop.* **2011**, *35*, 149–150. [[CrossRef](#)]
13. Khanuja, H.S.; Vakil, J.J.; Goddard, M.S.; Mont, M.A. Cementless femoral fixation in total hip arthroplasty. *J. Bone Jt. Surg. Am.* **2011**, *93*, 500–509. [[CrossRef](#)] [[PubMed](#)]
14. Brown, T.E.; Larson, B.; Shen, F.; Moskal, J.T. Thigh pain after cementless total hip arthroplasty: Evaluation and management. *J. Am. Acad. Orthop. Surg.* **2002**, *10*, 385–392. [[CrossRef](#)] [[PubMed](#)]
15. Engh, C.A., Jr.; Young, A.M.; Engh, C.A., Sr.; Hopper, R.H., Jr. Clinical consequences of stress shielding after porous-coated total hip arthroplasty. *Clin. Orthop. Relat. Res.* **2003**, *417*, 157–163. [[CrossRef](#)]
16. Lakstein, D.; Eliaz, N.; Levi, O.; Backstein, D.; Kosashvili, Y.; Safir, O.; Gross, A.E. Fracture of cementless femoral stems at the mid-stem junction in modular revision hip arthroplasty systems. *J. Bone Jt. Surg. Am.* **2011**, *93*, 57–65. [[CrossRef](#)] [[PubMed](#)]
17. Wilson, D.A.; Dunbar, M.J.; Amirault, J.D.; Farhat, Z. Early failure of a modular femoral neck total hip arthroplasty component: A case report. *J. Bone Jt. Surg. Am.* **2010**, *92*, 1514–1517. [[CrossRef](#)]
18. Quintana, J.M.; Arostegui, I.; Azkarate, J.; Goenaga, J.I.; Elexpe, X.; Letona, J.; Arcelay, A. Evaluation of explicit criteria for total hip joint replacement. *J. Clin. Epidemiol.* **2000**, *53*, 1200–1208. [[CrossRef](#)]
19. Gademan, M.G.J.; Hofstede, S.N.; Vlieland, T.P.M.V.; Nelissen, R.G.H.H.; De Mheen, P.J.M.-V. Indication criteria for total hip or knee arthroplasty in osteoarthritis: A state-of-the-science overview. *BMC Musculoskelet. Disord.* **2016**, *17*, 463. [[CrossRef](#)]
20. Lucchini, S.; Castagnini, F.; Giardina, F.; Tentoni, F.; Masetti, C.; Tassinari, E.; Bordini, B.; Traina, F. Cementless ceramic-on ceramic total hip arthroplasty in post-traumatic osteoarthritis after acetabular fracture: Long-term results. *Arch. Orthop. Trauma. Surg.* **2021**, *141*, 683–691. [[CrossRef](#)]
21. Fokter, S.K.; Levašič, V.; Kovač, S. The Innovation Trap: Modular Neck in Total Hip Arthroplasty. *ZdravVestn* **2017**, *86*, 115–126.

22. Aljenaei, F.; Catelas, I.; Louati, H.; Beaulé, P.E.; Nganbe, M. Effects of hip implant modular neck material and assembly method on fatigue life and distraction force. *J. Orthop. Res.* **2017**, *35*, 2023–2030. [[CrossRef](#)]
23. Zajc, J.; Moličnik, A.; Fokter, S.K. Dual Modular Titanium Alloy Femoral Stem Failure Mechanisms and Suggested Clinical Approaches. *Materials* **2021**, *14*, 3078. [[CrossRef](#)]
24. Weiser, M.C.; Chen, D.D. Revision for taper corrosion at the neck-body junction following total hip arthroplasty: Pearls and pitfalls. *Curr. Rev. Musculoskelet. Med.* **2016**, *9*, 75–83. [[CrossRef](#)]
25. Wright, C.G.; Sporer, S.; Urban, R.; Jacobs, J. Fracture of a Modular Femoral Neck After Total Hip Arthroplasty: A Case Report. *J. Bone Jt. Surg.* **2010**, *92*, 1518–1521.
26. Vucajnik, I.; Fokter, S.K. Modular Femoral Neck Fracture After Total Hip Arthroplasty. In *Recent Advances in Hip and Knee Arthroplasty*; IntechOpen: London, UK, 2012.
27. Grupp, T.M.; Weik, T.; Bloemer, W.; Knaebel, H.-P. Modular titanium alloy neck adapter failures in hip replacement—Failure mode analysis and influence of implant material. *BMC Musculoskelet. Disord.* **2010**, *11*, 3. [[CrossRef](#)]
28. Meftah, M.; Haleem, A.M.; Burn, M.B.; Smith, K.M.; Incavo, S.J. Early Corrosion-Related Failure of the Rejuvenate Modular Total Hip Replacement. *J. Bone Jt. Surg. Am.* **2014**, *96*, 481–487. [[CrossRef](#)]
29. Bernstein, D.T.; Meftah, M.; Paraniham, J.; Incavo, S.J. Eighty-six Percent Failure Rate of a Modular-Neck Femoral Stem Design at 3 to 5 Years: Lessons Learned. *J. Bone Jt. Surg.* **2016**, *98*, e49. [[CrossRef](#)]
30. Pipino, F. CFP Prosthetic Stem in Mini-Invasive Total Hip Arthroplasty. *J. Orthop. Traumatol.* **2004**, *4*, 165–171. [[CrossRef](#)]
31. Effenberger, H.; Heiland, A.; Ramsauer, T.; Plitz, W.; Dorn, U. A model for assessing the rotational stability of uncemented femoral implants. *Arch. Orthop. Trauma Surg.* **2001**, *121*, 60–64. [[CrossRef](#)]
32. Wolff, J. *Das Gesetz der Transformation der Knochen*; Verlag von August Hirschwald: Berlin, Germany, 1892.
33. Huiskes, R.; Weinans, H.; Van Rietbergen, B. The Relationship between Stress Shielding and Bone Resorption around Total Hip Stems and the Effects of Flexible Materials. *Clin. Orthop. Relat. Res.* **1992**, *274*, 124–134. [[CrossRef](#)]
34. Wang, X.; Xu, S.; Zhou, S.; Xu, W.; Leary, M.; Choong, P.; Qian, M.; Brandt, M.; Xie, Y.M. Topological Design and Additive Manufacturing of Porous Metals for Bone Scaffolds and Orthopaedic Implants: A Review. *Biomaterials* **2016**, *83*, 127–141. [[CrossRef](#)]
35. Diegel, P.D.; Daniels, A.U.; Dunn, H.K. Initial effect of collarless stem stiffness on femoral bone strain. *J. Arthroplast.* **1989**, *4*, 173–178. [[CrossRef](#)]
36. Fraldi, M.; Esposito, L.; Perrella, G.; Cutolo, A.; Cowin, S.C. Topological Optimization in Hip Prosthesis Design. *Biomech. Model. Mechanobiol.* **2010**, *9*, 389–402. [[CrossRef](#)]
37. Kappe, T.; Bieger, R.; Wernerus, D.; Reichel, H. Minimally Invasive Total Hip Arthroplasty trend or State of the Art? A Meta-analysis. *Der Orthopäde* **2011**, *40*, 774–780. [[CrossRef](#)]
38. Chen, W.C.; Lai, Y.S.; Cheng, C.K.; Chang, T.K. A cementless, proximally fixed anatomic femoral stem induces high micromotion with nontraumatic femoral avascular necrosis: A finite element study. *J. Orthop. Transl.* **2014**, *2*, 149–156. [[CrossRef](#)]
39. Bergmann, G.; Deuretzbacher, G.; Heller, M.; Graichen, F.; Rohlmann, A.; Strauss, J.; Duda, G.N. Hip contact forces and gait patterns from routine activities. *J. Biomech.* **2001**, *34*, 859–871. [[CrossRef](#)]
40. Naghavi, S.; Tamaddon, M.; Hejazi, M.; Moazen, M.; Liu, C. On the Mechanical Aspect of Additive Manufactured Polyether—Ether—Ketone Scaffold for Repair of Large Bone Defects. *Biomater. Transl.* **2022**, *3*, 142–151.
41. Svesnsson, N.L.; Valliappan, S.; Wood, R.D. Stress analysis of human femur with implanted Charnley prosthesis. *J. Biomech.* **1977**, *10*, 581–588. [[CrossRef](#)]
42. Papini, M.; Zdero, R.; Schemitsch, E.H.; Zalzal, P. The Biomechanics of Human Femurs in Axial and Torsional Loading: Comparison of Finite Element Analysis, Human Cadaveric Femurs, and Synthetic Femurs. *J. Biomech. Eng.* **2007**, *129*, 12–19. [[CrossRef](#)]
43. Tan, N.; van Arkel, R.J. Topology Optimisation for Compliant Hip Implant Design and Reduced Strain Shielding. *Materials* **2021**, *14*, 7184. [[CrossRef](#)]
44. Cortis, G.; Mileti, I.; Nalli, F.; Palermo, E.; Cortese, L. Additive Manufacturing Structural Redesign of Hip Prostheses for Stress-Shielding Reduction and Improved Functionality and Safety. *Mech. Mater.* **2022**, *165*, 104173. [[CrossRef](#)]
45. Mehboob, H.; Tarlochan, F.; Mehboob, A.; Chang, S.H.; Ramesh, S.; Harun, W.S.W.; Kadirgama, K. A Novel Design, Analysis and 3D Printing of Ti–6Al–4V Alloy Bio-Inspired Porous Femoral Stem. *J. Mater. Sci. Mater. Med.* **2020**, *31*, 104173. [[CrossRef](#)] [[PubMed](#)]
46. Kladovasilakis, N.; Tsongas, K.; Tzetzis, D. Finite Element Analysis of Orthopedic Hip Implant with Functionally Graded Bioinspired Lattice Structures. *Biomimetics* **2020**, *5*, 44. [[CrossRef](#)]
47. Engh, C.A.; Bobyn, J.D.; Glassman, A.H. Porous-coated hip replacement. The factors governing bone ingrowth, stress shielding, and clinical results. *J. Bone Jt. Surg. Br.* **1987**, *69*, 45. [[CrossRef](#)]
48. Gross, S.; Abel, E.W. A finite element analysis of hollow stemmed hip prostheses as a means of reducing stress shielding of the femur. *J. Biomech.* **2001**, *34*, 995–1003. [[CrossRef](#)] [[PubMed](#)]
49. Nunn, D.; Freeman, M.A.R.; Tanner, K.E.; Bonfield, W. Torsional stability of the femoral component of hip arthroplasty. Response to an anteriorly applied load. *J. Bone Jt. Surg. Br.* **1989**, *71*, 452–455. [[CrossRef](#)]
50. Freeman, M.A.R. Why resect the neck? *J. Bone Jt. Surg. Br.* **1986**, *68*, 346–349. [[CrossRef](#)] [[PubMed](#)]

51. Sugiyama, H.; Whiteside, L.A.; Engh, C.A. Torsional fixation of the femoral component in total hip arthroplasty. The effect of surgical press-fit technique. *Clin. Orthop.* **1992**, *275*, 187–193. [[CrossRef](#)]
52. Hanada, S.; Masahashi, N.; Jung, T.K.; Yamada, N.; Yamako, G.; Itoi, E. Fabrication of a High-Performance Hip Prosthetic Stem Using Ti-33.6Nb-4Sn. *J. Mech. Behav. Biomed. Mater.* **2014**, *30*, 140–149. [[CrossRef](#)]
53. Sun, C.; Wang, L.; Kang, J.; Li, D.; Jin, Z. Biomechanical Optimization of Elastic Modulus Distribution in Porous Femoral Stem for Artificial Hip Joints. *J. Bionic Eng.* **2018**, *15*, 693–702. [[CrossRef](#)]

**Disclaimer/Publisher's Note:** The statements, opinions and data contained in all publications are solely those of the individual author(s) and contributor(s) and not of MDPI and/or the editor(s). MDPI and/or the editor(s) disclaim responsibility for any injury to people or property resulting from any ideas, methods, instructions or products referred to in the content.